Polymer 49 (2008) 2686–2697

Contents lists available at ScienceDirect

Polymer

journal homepage: www.elsevier.com/locate/polymer

Compatibilized polymer blends with nanoscale or sub-micron dispersed phases achieved by hydrogen-bonding effects: Block copolymer vs blocky gradient copolymer addition

Jungki Kim [a,1], Robert W. Sandoval [a,1], Christine M. Dettmer [b], SonBinh T. Nguyen [b], John M. Torkelson [a,c,*]

[a] Department of Chemical and Biological Engineering, Northwestern University, Evanston, IL 60208, USA
[b] Department of Chemistry, Northwestern University, Evanston, IL 60208, USA
[c] Department of Materials Science and Engineering, Northwestern University, Evanston, IL 60208, USA

ARTICLE INFO

Article history:
Received 9 March 2008
Received in revised form 3 April 2008
Accepted 5 April 2008
Available online 10 April 2008

Keywords:
Styrene/hydroxystyrene copolymer
Compatibilization
Hydrogen bonding

ABSTRACT

Addition of styrene (S)/4-hydroxystyrene (HS) block, blocky gradient, or blocky random copolymer to 80/20 wt% polystyrene (PS)/polycaprolactone (PCL) blends is examined as a compatibilization strategy. Four copolymers are synthesized by controlled radical polymerization, each with an S block and the other block being a HS block or S/HS random or gradient copolymer. Compatibilization depends on copolymer level and HS sequence distribution and content. Using a two-step solution-mixing/melt-mixing process, addition of 2 wt% and 5 wt% nearly symmetric S/HS diblock copolymer leads to compatibilization with average PCL domain diameters of 390–490 nm and 90–110 nm, respectively. In contrast, adding 0.25–0.75 wt% copolymer leads to microscale dispersed-phase domains and only reduced melt-state coarsening. Results with 2–5 wt% added copolymer indicate that a major reduction in interfacial tension is facilitated by hydrogen bonding of HS units and PCL carbonyl groups. Nanoscale confinement of normally semi-crystalline PCL within blends with 100 nm dispersed phases impedes PCL crystallizability, yielding liquid-state PCL domains at room temperature and demonstrating that properties of nanostructured blends and microstructured blends can differ greatly. Polystyrene/PCL blends are also made by one-step melt mixing with low mol% HS copolymers. Adding 5 wt% blocky gradient S/HS copolymer (86/14 mol% S/HS) leads to compatibilization with an average dispersed-phase diameter of 360–420 nm. In contrast, adding 5 wt% blocky random (87/13 mol% S/HS) or 5 wt% diblock (81/19 mol% S/HS) copolymer yields microscale dispersed-phase domains and only reduced coarsening. Crystallization in these blends is less hindered than in blends containing 2–5 wt% nearly symmetric S/HS diblock copolymer, indicating that both hydrogen bonding and confinement suppress PCL crystallization.

1. Introduction

Production of polymer blends is an attractive, economical way to obtain tunable, synergistic material properties using currently available materials. In order to obtain desired properties from immiscible polymer blends, it is often necessary to produce a dispersed phase with an average domain diameter under a certain size typically less than a few microns [1–4]. Substantial interest has recently been focused on the production of immiscible blends in which the dispersed-phase domain size or the length scales associated with co-continuous blends approach or are at the nanoscale [5–12]. Stabilization of nanoscale or sub-micron domain sizes against coarsening during melt processing, which is the scientific criterion for compatibilization [13], is an important challenge in the processing of polymer blends.

Achieving compatibilized, nanoscale, immiscible blends by melt mixing is problematic because of the dependence of the dispersed-phase size on a variety of factors [14–17]: the ratio of the deforming viscous stress (the product of matrix viscosity and shear rate in the case of simple shear flow) to the resisting interfacial stress (the ratio of interfacial tension to droplet radius); the ratio of dispersed-phase viscosity to matrix viscosity; interfacial mobility, viscoelastic effects, and volume fraction of the dispersed phase, all of which affect the likelihood of coalescence; and the shear rates and extensional flow effects present in melt mixing. As a result, the minimum average dispersed-domain size achieved during normal melt mixing of immiscible blends is often ~1 μm in optimal cases (and rarely significantly below ~500 nm in the absence of reactive compatibilization at long mixing times [18]) and substantially

---

[*] Corresponding author. Department of Chemical and Biological Engineering, Northwestern University, 2145 Sheridan Road, Evanston, IL 60208-3120, USA.
E-mail address: j-torkelson@northwestern.edu (J.M. Torkelson).
[1] Co-first authors.

0032-3861/$ – see front matter © 2008 Elsevier Ltd. All rights reserved.
doi:10.1016/j.polymer.2008.04.008

higher in blends with a large mismatch in component viscosities. Thus, the production of dispersed-phase domain sizes in immiscible blends at or near the nanoscale is challenging.

Many blend compatibilization strategies have been studied [3]. Among these include reactive compatibilization in which interfacial block copolymer is produced from interpolymer condensation-type reactions during melt processing [19–21] or interpolymer radical reactions during solid-state shear pulverization [22,23]. Other strategies involve adding block copolymers [13,14,24–27], tapered block copolymers [28–30], graft copolymers [31,32], or gradient copolymers [12,33–36] to the blend to serve as compatibilizers. Besides improving interfacial adhesion, such copolymers can reduce interfacial tension and yield steric effects that stabilize the dispersed phase against coalescence [11–14,17–43].

Here we investigate the production of compatibilized, immiscible blends with dispersed-phase domains at or near the nanoscale. We employ as interfacial compatibilizers various types of styrene/4-hydroxystyrene (S/HS; also known as styrene/4-vinylphenol) block copolymers, each consisting of a block of polystyrene (PS) and the other block of pure HS polymer or S/HS copolymer. These compatibilizers are added at low levels ($\leq$5 wt%) during melt mixing of 80/20 wt% PS/polycaprolactone (PCL) blends. Styrene/4-hydroxystyrene copolymers can be produced by hydrolysis of styrene/4-acetoxystyrene (S/AS) copolymers made by controlled radical polymerization (CRP) [34,44–46], with CRP being a simple synthesis approach [47–50] that makes S/HS copolymers amenable to scientific study and application. The hydroxyl groups in the HS units can hydrogen bond with carbonyl groups within the PCL [51–58]. Specifically, Kuo and Chang have demonstrated miscibility between PCL and S/HS copolymers using FTIR spectroscopy [58].

Our recent study [34] found that addition of S/HS gradient copolymer was more effective for compatibilizing 80/20 wt% PS/PCL blends than random copolymers of similar molecular weight and composition. When the HS content of the gradient copolymer was increased from 41 mol% to 75 mol%, the impact of the copolymer on interfacial tension was strongly reduced (i.e., PCL domain size in blends without copolymer was nearly identical to those in blends containing 5 wt% of 25/75 mol% S/HS gradient copolymer). With the higher HS content, the copolymer can be 'pulled' into the PCL phase due to the increase of hydrogen-bonding (H-bonding) units, leading to an uneven interfacial coverage and the inability of the copolymer to strongly alter the interfacial tension. The study described here examines the compatibilization efficiency of S/HS copolymers with dramatically different copolymer architecture than in our previous study. The copolymers employed here contain relatively long S blocks. In three of four cases, the copolymers have HS contents less than 20 mol%. Two of the four copolymers are S/HS diblock copolymers, one is a 'blocky' gradient copolymer consisting of an S block and a second block which is an S/HS gradient copolymer, and another is a 'blocky' random copolymer consisting of one S block and a second block which is an S/HS random copolymer. (Examples of studies in which blocky gradient and blocky random copolymers have been made by controlled radical polymerization include Refs. [44,49,50].) These major differences in copolymer structure significantly affect the efficacy of compatibilization.

Our investigation differs from the heavily studied approach of inducing blend miscibility by introducing H-bonding moieties into one of the polymers constituting an immiscible blend in its unmodified state [58–64]. (For reviews of H-bonding in blends, see Refs. [51,52,59].) Instead, our approach is influenced by compatibilization studies [34,42,65,66] that have added S/HS copolymers capable of H-bonding with a polymer in the immiscible blends. For example, Zhao et al. [65] observed reduced domain sizes in solution-cast PS/poly(ethyl oxazoline) blends upon addition of small levels of a 50/50 wt% S/HS block copolymer, albeit leading to dispersed-phase domain sizes near 10 μm or larger. Edgecombe et al. [42] also compared the compatibilizing abilities of various S/HS copolymers (random, graft and block) in PS/poly(4-vinyl pyridine) (PVP) blends and demonstrated that HS groups were effective in anchoring into the PVP phase, leading to H-bond formation and contributing to interfacial pull-out resistance.

We substantiate the strong compatibilizing effect of the S/HS block copolymers via high-resolution electron microscopy of the micro/nanostructure in the melt-processed PS/PCL blend as a function of static high-temperature annealing time and take advantage of the fact that the dispersed-phase melting/crystallization behavior can be modified dramatically when its domain size is confined at or near the nanoscale [11,17,18,67–73]. The latter point can be important in tuning the properties of immiscible blends with a crystallizable minor phase. We also examine the effects of the level of S/HS copolymer on compatibilization and PCL crystallizability in these blends. It is also noteworthy that irregular, non-spherical dispersed-phased domains are formed in 80/20 wt% PS/PCL blends compatibilized with 5 wt% S/HS block copolymers, which remain stable during long-term high-temperature annealing.

2. Experimental section

2.1. Materials and methods

Styrene (Aldrich, 99%) and 4-acetoxystyrene (Aldrich, 96%) were deinhibited using *tert*-butylcatechol inhibitor remover and dried over CaH_2. The unimolecular initiator alkoxyamine 29 (2,2,5-trimethyl-3-(1-phenylethoxy)-4-phenyl-3-azahexane) was synthesized as previously reported [33,74]. Polystyrene (Pressure Chemical; nominal molecular weight (MW) = 30,000, $M_w/M_n \leq 1.06$) and PCL (Aldrich; $M_n = 110,000$ g/mol and $M_w/M_n = 1.80$ relative to PS calibration) were used as-received. The M_n and M_w values of the (co)polymers and the commercially available PCL were determined by gel permeation chromatography (GPC, Waters Breeze) calibrated with PS standards using tetrahydrofuran (THF) as eluent. Each S/AS copolymer composition was measured by ^1H NMR spectroscopy (Varian Inova 500 MHz) using $CDCl_3$ as solvent. NMR peaks associated with aromatic hydrogens (m, 9H, 6.2–7.3 ppm) and with other hydrogens (m, 9H, 1.2–2.4 ppm) were compared to determine the styrene mole fraction (F_S).

2.2. Synthesis of copolymers

All S/HS copolymers were synthesized by controlled radical polymerization of S/AS copolymers followed by hydrolysis (see Refs. [34,44–46] for related synthesis procedures of S/HS copolymers). For the two S/AS diblock copolymers with F_S values of 0.56 (B56) and 0.81 (B81) as determined by ^1H NMR, the two-step chain extension process was employed. The procedure for B56 preparation is described elsewhere [46]. For B81, the PS macroinitiator was synthesized by combining S (16 mL; 0.140 mol) and alkoxyamine 29 (15 μL; 3.92×10^{-3} mol/L) in a test tube, purging the tube with N_2 for 30 min, and reacting for 2 h at 115 °C. The resulting PS ($M_n = 38,000$ g/mol; $M_w/M_n = 1.30$) was isolated by washing via several cycles of dissolution in THF and precipitation in methanol followed by drying under vacuum for a day. The second step involves chain extension of the PS macroinitiator. The PS macroinitiator (0.5 g) was dissolved in AS (1.5 mL; 9.81×10^{-3} mol) and purged with N_2 for 30 min, and was then reacted for 30 min at 115 °C. The resulting S/AS block copolymer was washed and dried.

A semi-batch chain extension reaction was used to create S/AS 'blocky' gradient and 'blocky' random copolymers. The 'blocky' gradient copolymer was synthesized by combining S (10 mL; 0.0874 mol) and alkoxyamine 29 (20 μL; 5.23×10^{-3} mol/L) in a test tube. The tube was sealed with a rubber stopper, purged with N_2 for

30 min, and immersed into an oil bath at 115 °C. After 2 h, an aliquot (~1 mL) was taken for GPC analysis. A needle was then inserted into the tube, and AS was added continuously at a rate of 2 mL/h for 3 h in order to increase the AS concentration in the comonomer mixture. The reaction was quenched and the resulting S/AS copolymer was washed and dried as described above. The PS block in the copolymer (obtained from the aliquot) was found by GPC to have $M_n = 44{,}800$ g/mol and $M_w/M_n = 1.60$, and the final S/AS 'blocky' gradient copolymer was found to have an apparent $M_n = 56{,}600$ g/mol and $M_w/M_n = 1.60$ by GPC and $F_S = 0.86$ by ^{1}H NMR analysis.

The 'blocky' random copolymer was synthesized with a slightly modified method. Styrene (16 mL; 0.140 mol) and alkoxyamine 29 (15 μL; 3.92×10^{-3} mol/L) were combined, sealed in a test tube, and purged with N_2 for 30 min, followed by immersion into an oil bath at 115 °C. After 2 h, an aliquot (~1 mL) was taken for analysis. Next, 5 mL of AS was added, and the reaction continued for another 2 h, followed by quenching, cleaning, and drying of the copolymer. The PS block in the copolymer had $M_n = 37{,}000$ g/mol and $M_w/M_n = 1.30$; the 'blocky' random copolymer had an apparent $M_n = 58{,}000$ g/mol, $M_w/M_n = 1.30$, and $F_S = 0.87$.

The S/AS copolymers were hydrolyzed as previously reported [34,44–46] by dissolution in 9:1 v/v 1,4-dioxane/hydrazine hydrate mixtures that were stirred at 22 °C under N_2 for 6 h. The resulting S/HS copolymers were washed repeatedly with deionized water and dried in a fume hood overnight and then under vacuum for 2–3 days. Analysis by ^{1}H NMR confirmed complete hydrolysis with the loss of the acetoxy hydrogen peak near 2.28 ppm. Fig. 1 and Table 1 provide schematic illustrations and characterization.

2.3. Thermal analysis of S/HS copolymers

Thermal analysis was done by differential scanning calorimetry (DSC, Mettler–Toledo DSC 822e, calibrated with an indium standard) using a sample mass of 3–7 mg. Dry N_2 was passed (50–55 mL/min) through the DSC cell during measurement. Each S/HS copolymer sample was heated at a rate of 10 °C/min to 210 °C and held at that temperature for 15 min to erase thermal history. Then samples were cooled to 25 °C at a rate of 40 °C/min and reheated at 10 °C/min. The second heat data were used to determine glass transition temperatures (T_gs).

2.4. Melt processing of PS/PCL blends

The 80/20 wt% PS/PCL blends were prepared in two ways. A two-step process was used for blends containing B56: a total of 0.80 g of dry polymer mixture was dissolved in 1,4-dioxane followed by precipitation with rapidly stirred methanol. A powdery precipitate was isolated and dried under vacuum at 60 °C for a day and further dried at 120 °C under vacuum for a few hours to remove residual solvent. Melt processing of each pre-mixed blend was done at 210 °C in a cup-and-rotor mixer (Atlas Electronic Devices Mini-MAX molder) for 5 min at 120 rpm with three steel balls in the cup to ensure intense mixing [13,21]. (Based on the resulting dispersed-phase domain size, Maric and Macosko [75] have shown that melt mixing of immiscible polymer blends with a MiniMAX mixer containing three small steel balls can yield blend microstructures that are comparable to those attained with internal, intensive batch mixers and twin-screw extruders.) Samples collected by spatula were quenched in liquid N_2. Static high-temperature annealing (30–40 mg samples) was done in DSC by holding at 210 °C for 30 min, 90 min or 240 min.

Fig. 1. Schematic illustration of styrene (S)/hydroxystyrene (HS) copolymers used as compatibilizers for PS/PCL melt blends. B56: a symmetric S/HS diblock copolymer consisting of one S block and one HS block, BR87: a diblock copolymer consisting of one S block and one short block of S/HS random copolymer, BG86: a diblock copolymer consisting of one S block and one short block of S/HS gradient copolymer, and B81: an asymmetric S/HS diblock copolymer consisting of one S block and one short HS block.

Table 1
Characterization data of S/HS copolymers synthesized by controlled radical polymerization

Sample ID	Description	M_n (g/mol)	F_S[c]	PS block M_n[b] (g/mol)
B56	S/HS diblock (symmetric)	78 200[a]	0.56	35 200
BR87	PS block + short block of S/HS random	58 000[b]	0.87	37 000
BG86	PS block + short block of S/HS gradient	56 600[b]	0.86	44 800
B81	S/HS diblock (PS block + short HS block)	51 900[a]	0.81	38 000

[a] Determined by M_n of PS block and F_S value of S/AS precursors.
[b] Determined by GPC relative to PS standards.
[c] Styrene mole fraction in copolymer (determined by NMR).

Blends containing highly asymmetric S/HS copolymers (BR87, BG86 and B81; see Table 1) were prepared by one-step melt mixing in the MiniMAX. Dry polymer mixture (PS + PCL + S/HS copolymers) with 5 wt% S/HS copolymer was inserted in the cup, and mixing was done at 210 °C for 10 min at 120 rpm. Collection and annealing (30 min, 100 min and 240 min at 210 °C) of samples were done as described above. PS/PCL (90/10 wt%) blends, both without copolymer and with 5 wt% BG86, were similarly prepared by one-step melt mixing.

2.5. Electron microscopy of PS/PCL blends

Scanning electron microscopy (SEM) samples were obtained by cryo-fracturing in liquid N_2 and etching in acetic acid to remove the dispersed PCL phase. A layer of Au/Pd (3–5 nm) was coated onto the surface, and the morphology was observed using a Hitachi S4500 SEM (5 keV) equipped with a cold field emission gun. At least 250 dispersed-phase domains per sample were analyzed after digitization of each image, and image analysis software (Scion Image Beta 4.0.2; ImageJ 1.36b) was used to determine the number-average dispersed-phase diameter (D_n). When the dispersed-phase domain was non-spherical, the calculated diameter was that of a circle with same area, as determined from 2-D image analysis by the software. In order to assess quantitatively the distribution of dispersed PCL domain sizes, a ratio of D_{vs} (volume-weighted particle size/area-weighted particle size) to D_n was calculated for each sample.

2.6. Thermal analysis of PS/PCL blends: crystallization and melting of PCL phase

For PCL crystallization and melting characterization, a 5–10 mg DSC sample of each PS/PCL blend was heated to 210 °C and held for 30 min to erase thermal history. Samples were then cooled to −70 °C at a rate of 10 °C/min to obtain non-isothermal crystallization curves and held at −70 °C for 3 min before being reheated to 210 °C at a rate of 10 °C/min to obtain melting curves. For room-temperature annealing of PS/PCL blends containing B81, each DSC sample was first heated to 210 °C and held for 30 min to erase thermal history. The DSC samples were then cooled to 25 °C and stored in glass vials at room temperature for 40 days. After storage, DSC samples were reheated at 10 °C/min to obtain PCL melting curves.

2.7. FTIR measurements on blend samples

Blends containing different S/HS copolymers as well as the neat PS/PCL blend were analyzed by FTIR. Each blend was mixed with KBr powder to form a thin disc, and FTIR spectra were collected with a Nexus 670 FTIR (ThermoNicolet) instrument at room temperature.

3. Results and discussion

3.1. Preparation of S/HS copolymers and characterization of glass transition temperatures

Fig. 1 schematically illustrates the S/HS copolymer structures, and Table 1 summarizes the characterization data. All four S/HS copolymers are "diblocks". However, while each contains an S block, there are significant differences in the distribution of S/HS comonomers or the overall S mole fraction within the copolymers, resulting from different controlled radical polymerization conditions. For the blocky random copolymer with overall $F_S = 0.87$ (BR87), S was charged in a test tube and began to undergo polymerization, and after a set time a pulse of AS (later hydrolyzed in the copolymer to HS) was added. Since the S/AS reactivity ratios are close to unity [76] and copolymerization was done at low conversion, the average sequence distribution remained constant along the random copolymer portion of the chain. The mole fraction of AS units in the random block of the copolymer was determined to be 0.41. For the blocky gradient copolymer synthesis with $F_S = 0.86$ (BG86), after a fixed time of S polymerization, AS was added to the test tube at a low, continuous rate, increasing the AS content in the comonomer mix over time and thereby the AS content (later hydrolyzed in the copolymer to HS) along the gradient copolymer portion of the chain. Aliquots were collected during polymerization of the gradient block in the BG86 copolymer, and the cumulative S mole fraction decreased as the copolymer molecular weight increased, in accord with expectations. For example, after 2 h reaction time (and just prior to AS addition) the blocky gradient copolymer had $F_S = 1.00$ and $M_n = 44{,}800$ g/mol, after 4 h reaction time (and after AS addition to the semi-batch reactor) the copolymer had $F_S = 0.93$ and apparent $M_n = 50{,}800$ g/mol, and after 5 h reaction time the copolymer had $F_S = 0.87$ and apparent $M_n = 58{,}000$ g/mol.

Fig. 2 shows DSC heat curves for the four S/HS copolymers. The nearly symmetric diblock copolymer, B56, exhibits two distinct T_gs corresponding to well-segregated lamellar microphases consisting of nearly pure S ($T_g = 100$ °C) or nearly pure HS ($T_g = 190$ °C) regions. While the other three copolymers containing low levels of HS show a common T_g near 100 °C corresponding to the PS block, the locations and strengths of the second, higher T_gs (noted by arrows in Fig. 2) differ depending on the nature of the second block. The BR87 copolymer exhibits a second T_g at ~115–120 °C associated with a random distribution of S and HS units in the second block which is lean in HS units. The DSC heat curve for the BG86 copolymer shows a second T_g near 160 °C, corresponding to the second block comprised of an S/HS gradient distribution of S/HS that is relatively rich in HS units and in accord with previous T_g characterization of S/HS gradient copolymers [44,46]. The asymmetric B81 diblock copolymer yields a second T_g near 190 °C that is associated with HS nanodomains and is much weaker than that exhibited by the nearly symmetric B56 diblock copolymer.

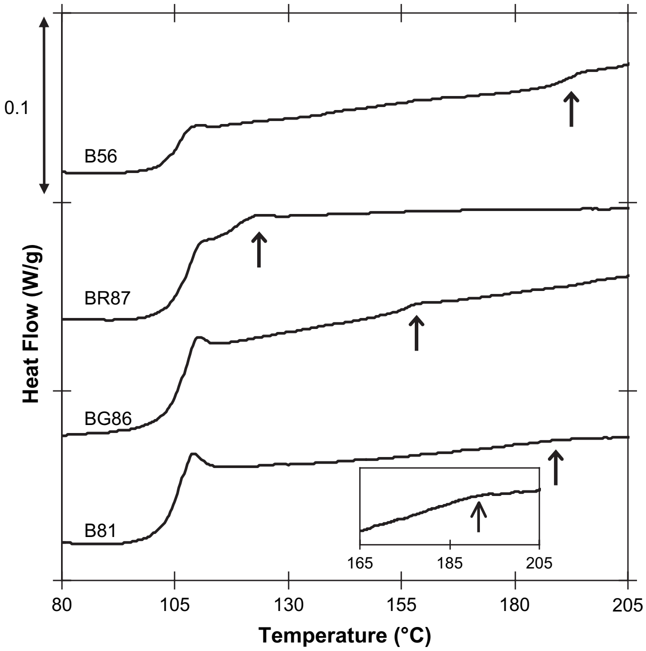

Fig. 2. DSC thermograms (heating rate = 10 °C/min) for T_g characterization of the S/HS copolymers (the arrows below each curve indicate the location of the second T_g). The inset is a magnification of the heat curve of B81 near the second T_g region.

3.2. Two-step compatibilization of PS/PCL blends by melt processing: effect of the amount of H-bonding S/HS diblock copolymer (B56) added as interfacial compatibilizer

Each blend contains 80 wt% PS (PS homopolymer + S block in B56) with a varying amount of B56 (0–5 wt% with respect to the total blend) added to the PS/PCL blend. In addition to the T_g from the PS block at 100 °C, the B56 copolymer has a second, strong T_g at 190 °C, which prevents effective melt mixing of the copolymer when added directly to the blend. As a result, we used a two-step mixing protocol involving solution premixing of all components (PS/PCL and B56) followed by melt mixing in order to disperse B56 within each blend [34].

Fig. 3 shows electron micrographs of melt-mixed PS/PCL + B56 blends before and after static annealing at 210 °C for 240 min. The morphologies resulting from melt mixing exhibit a sharp reduction in the dispersed PCL domain sizes with increasing B56 content. Because of the nanoscale nature of the dispersed-phase domains in the blend containing 5 wt% B56, we also shown in Fig. 4 the micrographs at much higher magnification.

Several points are evident from Figs. 3 and 4 and related micrographs. First, the dispersed-phase domain diameters can be tuned from the microscale (with 0.25 wt% B56, the number-average dispersed-phase diameter (D_n) > 2 μm) to the nanoscale (with 5 wt% B56, $D_n = 90$–110 nm) by addition of sufficient diblock copolymer. This is consistent with the notion that the S/HS diblock copolymer at the blend interfacial regions leads to a significant reduction in interfacial tension, with larger reductions occurring at higher diblock copolymer content. These results are in sharp contrast with our previous study employing S/HS gradient copolymers as compatibilizers of 80/20 wt% PS/PCL blends which were made by the same homopolymers and two-step mixing process employed here. The addition of 5 wt% of 59/41 mol% S/HS gradient copolymer resulted in $D_n = 1.62$ μm while the addition of 5 wt% of 25/75 mol% S/HS gradient copolymer resulted in $D_n = 2.72$ μm, both values more than an order of magnitude larger than that obtained upon the addition of 5 wt% B56. Second, for the blend with 5 wt% B56, a significant fraction of the nanoscale dispersed phase is

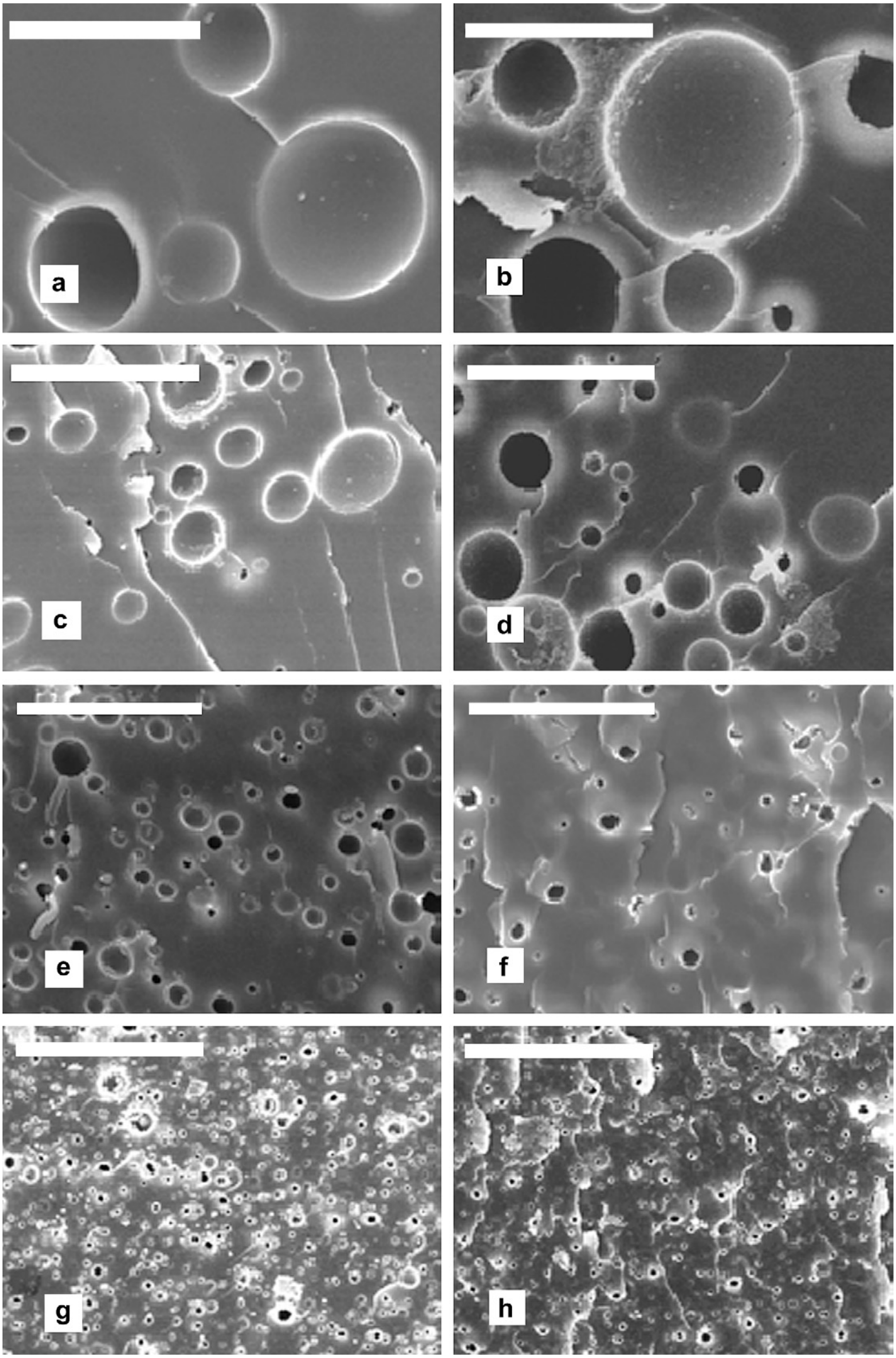

Fig. 3. Scanning electron micrographs of 80/20 wt% PS/PCL blends with added B56 before and after annealing for 240 min at 210 °C: blend with 0.25 wt% B56 before (a) and after (b) annealing; blend with 0.75 wt% B56 before (c) and after (d) annealing; blend with 2 wt% B56 before (e) and after (f) annealing; blend with 5 wt% B56 before (g) and after (h) annealing. The size bars represent 5 μm.

non-spherical and retains a non-spherical shape after long-term, high-temperature annealing. This is consistent with a nearly vanishing interfacial tension in the blend containing 5 wt% B56, an effect that has been rarely reported in the literature [34,39]. We also note that crosslinking via condensation reaction between hydroxyl groups on different HS repeat units in the interfacial regions

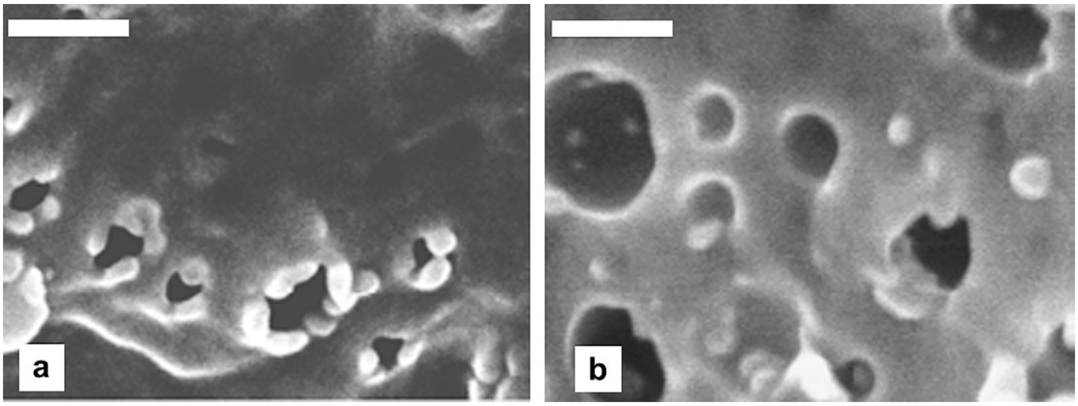

Fig. 4. Scanning electron micrographs of irregularly shaped PCL domains in the 80/20 wt% PS/PCL blend with 5 wt% B56 before (a) and after (b) annealing for 240 min at 210 °C. The size bars represent 250 nm.

is possible at the high-temperature annealing conditions used to study compatibilization [77], which would aid in stabilizing the unusual non-spherical dispersed-phase domain shapes observed in Fig. 4. Third, blends containing 2–5 wt% B56 are fully compatibilized, i.e., there is no growth observed in D_n with high-temperature static annealing. Thus, there is sufficient steric hindrance provided by interfacial block copolymer to prevent coalescence.

Table 2 and Fig. 5 show the data associated with our characterization of dispersed-phase domains in blends to which B56 diblock copolymer was added. For non-compatibilized blends, D_n is expected to obey the following equation as a function of annealing time, t [78–80]:

$$D_n^3(t) = D_n^3(0) + Kt \qquad (1)$$

where $D_n(0)$ is the value of D_n upon removal of the blend from the mixer (before static annealing) and K is the coarsening rate parameter. (Our value of K differs by a factor of 8 from that described by Crist and Nesarikar [78] because their equation involves the cube of the average radius.) Eq. (1) is valid for coarsening by coalescence and/or Ostwald ripening. Fig. 5 shows that within error K is zero for blends containing 2–5 wt% B56 diblock copolymer. Eq. (1) does not adequately describe the coarsening for the blend with 0.25 wt% B56, the lowest amount of diblock copolymer. It is possible that the near invariance of D_n^3 in that system at annealing times of 30–240 min is because once some coarsening has occurred within the first 30 min, there may be sufficient interfacial copolymer to prevent further coarsening. This effect has been previously reported with block copolymer addition to immiscible blends [27].

The D_{vs}/D_n values in Table 2 indicate that the smallest polydispersity in dispersed-phase domain size occurs in the 2 wt% B56 blend. This is consistent with the idea that the copolymer coverage of the interfacial regions is greatest and most even in this system. It is possible that the larger D_{vs}/D_n values obtained in the blend containing 5 wt% B56 may be due in part to the nanoscopic scale of the dispersed phases, creating somewhat greater error in these values.

Table 2
Average PCL domain sizes obtained via SEM image analysis in 80/20 wt% PS/PCL blends with added B56: effects of annealing time at 210 °C and B56 addition level

B56 addition level (wt%)	0 min annealing		30 min annealing		90 min annealing		240 min annealing	
	D_n (μm)	D_{vs}[a]/D_n	D_n (μm)	D_{vs}/D_n	D_n (μm)	D_{vs}/D_n	D_n (μm)	D_{vs}/D_n
0.25	2.44	1.61	2.97	1.53	2.90	1.39	3.05	1.85
0.75	1.00	1.81	0.97	1.73	0.91	2.00	1.67	1.50
2	0.49	1.16	0.39	1.26	0.46	1.21	0.39	1.30
5	0.11	1.62	0.09	1.30	0.10	1.86	0.10	1.56

[a] $D_{vs} = \sum(D_n^3)/\sum(D_n^2)$ and represents the ratio of the volume-weighted average diameter to area-weighted average diameter; thus, the ratio D_{vs}/D_n provides a quantitative indication of the polydispersity in dispersed-phase domain sizes.

In our previous study of PS/PCL blends employing S/HS gradient copolymers as compatibilizers [34], we reported that H-bonding between the S/HS copolymers and PCL reduced the crystallization and melting temperatures as well as the enthalpies of crystallization and melting of the dispersed PCL phases. In our current study of PS/PCL blends with S/HS B56 as compatibilizer, we have followed the approach of Kuo and Chang [58] for determining the presence of H-bonds between the hydroxyl group in HS and the PCL carbonyl group via the appearance of a band at 1708 cm^{-1} in an FTIR spectrum. In our blend containing 5 wt% B56 and therefore less than 1 wt% hydroxyl groups, we observed a shoulder peak near 1708 cm^{-1} that is absent in the PS/PCL blend without copolymer. Thus, our PS/PCL blends containing B56 have H-bonds which may suppress PCL crystallization. Others investigating the miscibility of PCL with (co)polymers containing HS, and thereby presumed to result in blends with H-bonds, have reported significant reductions in PCL crystallinity and/or melting point [51–58]. Nanoscale phase-segregated PS/PCL blends [9] made by non-interfering simultaneous PS and PCL polymerization (and lacking H-bonds) also resulted in a reduced crystallinity of the minor PCL phase relative to neat PCL. As our blend containing 5 wt% B56 block copolymer has both nanoscale PCL domains and H-bonds, it is easy to hypothesize that such a blend may exhibit dramatically different crystallinity compared with PS/PCL blends without copolymer.

Fig. 6 shows the effect of B56 content on the non-isothermal crystallization of PS/PCL blends. All blends exhibit reduced peak crystallization temperatures compared to neat PCL. With blends containing less than 1 wt% B56, the reduction in PCL crystallization temperature, measured by onset or peak temperature, is 1–3 °C, with peak temperatures exceeding 30 °C. The effect is very large in blends containing 2–5 wt% B56, with little or no crystallization evident at room temperature and crystallization peak temperatures of −15 °C to −35 °C. The large effects in blends containing 2–5 wt% B56 are expected from two standpoints. First, any H-bonds between hydroxyl groups in the interfacial B56 copolymer and the PCL in dispersed domains would interfere with or slow the frontal growth of crystallizing spherulites, hindering PCL crystallization [52,81]. Second, because these blends yield many PCL domains in the ~100 nm size range, a reduced crystallizability is expected due to confined or fractionated crystallization [11,17,18,67–73]. (Confined crystallization occurs when the crystallizable domain is at or near the nanoscale and contains no heterogeneity that nucleates crystallization at the normal bulk crystallization temperature. Instead, the confined domain nucleates at a lower supercooling, either from a heterogeneity active at that supercooling or homogeneously.)

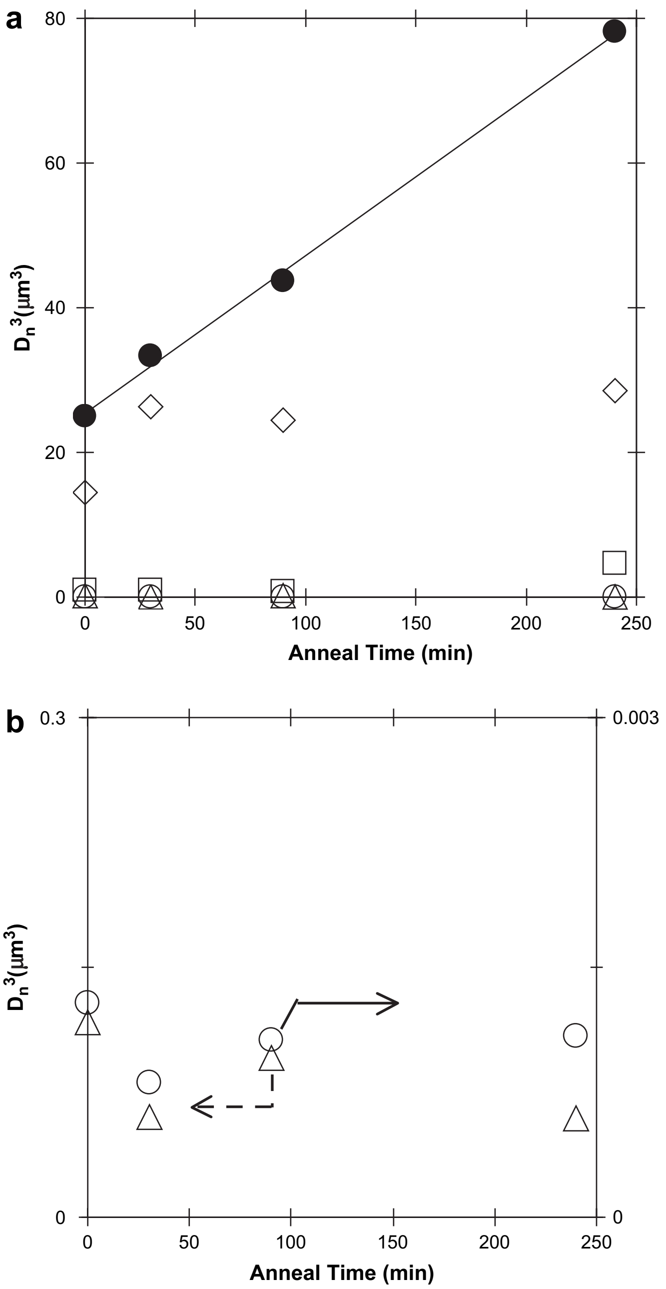

Fig. 5. (a) Effect of annealing time on D_n^3 for 80/20 wt% PS/PCL blends by two-step processing: blend without added copolymer (filled circles), blend with 0.25 wt% B56 addition (open diamonds), blend with 0.75 wt% B56 addition (open squares), blend with 2 wt% B56 addition (open triangles), and blend with 5 wt% B56 addition (open circles). (b) Magnification of (a) for the lower D_n^3 values associated with the results from the blends containing 2 wt% (referred to the left axis; open triangles) and 5 wt% (referred to the right axis; open circles) B56.

The effects of compatibilization and the nanoscopic nature of the dispersed PCL phases on blend properties are starkly manifested by attempts to achieve isothermal crystallization of PCL nanodomains at room temperature. Because room-temperature crystallization of blends with 2–5 wt% B56 is extremely slow, no enthalpy change can be measured during isothermal, room-temperature annealing in the DSC. To examine the possibility of long-term room-temperature crystallization, samples were first heated in order to melt any crystallites and then rapidly cooled to room temperature (~22 °C) where they were stored outside a DSC for 40 days. After storage, melting characteristics were measured via DSC heating curves given in Fig. 7.

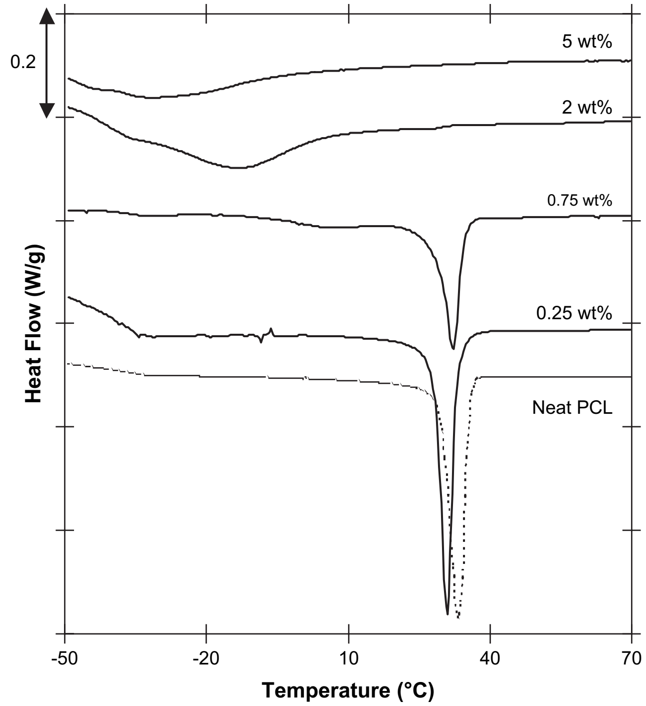

Fig. 6. Non-isothermal crystallization (cooling rate = 10 °C/min) thermograms of PCL domains in the 80/20 wt% PS/PCL blends containing B56. Also shown is a thermogram obtained from neat PCL sample (dotted curve; the DSC signal was multiplied by 0.2 to adjust the scale).

Blends containing 0.25–0.75 wt% B56 and subjected to 40 days of room-temperature annealing exhibit large melting peaks characteristic of semi-crystalline PCL. However, blends with 2–5 wt% B56 exhibit melting peaks with vastly reduced integrated areas. In particular, the melting peak is negligibly small for the blend with 5 wt% B56, meaning that the dispersed PCL phases remain

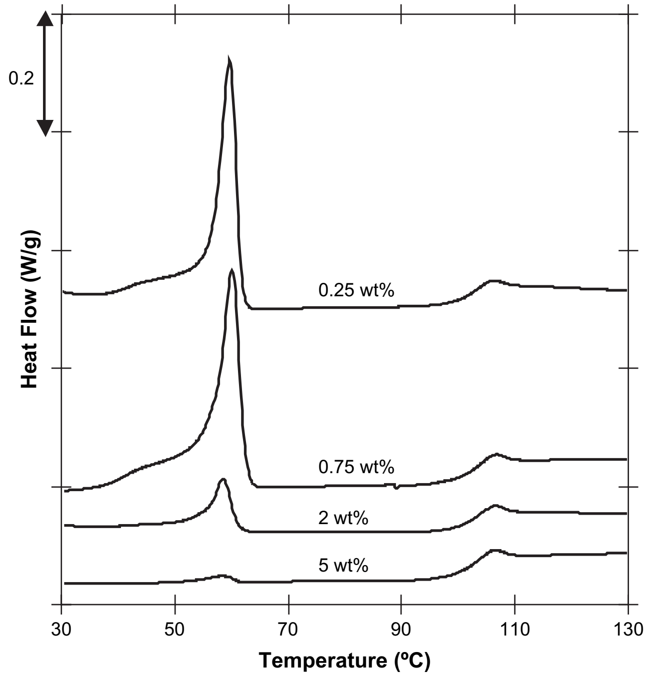

Fig. 7. DSC heating curves (10 °C/min) for characterization of PCL melting in 80/20 wt% PS/PCL blends containing B56. Prior to heating, the samples had been annealed for 30 min at 210 °C, then quenched to room temperature and annealed at room temperature for 40 days.

amorphous at extremely long times at room temperature. The combined confined crystallization and H-bonding lead to an almost total arrest of crystallization, meaning that, at room temperature, this compatibilized PS/PCL blend is not a glassy/semi-crystalline blend but rather a glassy/liquid blend. This shows very simply how nanostructured blends can have properties that differ greatly from those of microstructured blends.

3.3. One-step melt processing of blends: compatibilization by different types of S/HS copolymers with low HS contents

The results above indicate that, with appropriate levels of mixing, nearly symmetric S/HS block copolymers can compatibilize PS/PCL blends. However, the two-step mixing protocol required for blends containing B56 block copolymer (necessitated by the high, strong T_g of the HS block within B56, resulting from HS-unit association [51,81–83]) is neither environmentally green nor commercially friendly due to its first solvent-based mixing step.

In order to achieve one-step, effective melt mixing (without a solvent-based mixing step) with the potential to lead to compatibilized PS/PCL blends, we synthesized three S/HS copolymers with similar, low HS mole fractions (high F_S values), each with an S block of length similar to B56 (see Table 1). These blocky S/HS copolymers differ by the distribution of HS units in the second block. As Table 1 and Fig. 1 indicate, the BR87, BG86, and B81 copolymers each contain a second "block" consisting of an S/HS random copolymer, an S/HS gradient copolymer, or a short HS block, respectively. Because B81 block copolymer is only 19 mol% HS, in bulk it exhibits a barely perceptible T_g at ~190 °C. Thus, in contrast to the B56 copolymer which exhibits little or no dispersion during one-step melt mixing at 5 wt% in a PS/PCL blend, 5 wt% B81 copolymer can be dispersed in the PS/PCL blend using one-step melt mixing. The considerably lower values for the second T_gs obtained in the BR87 and BG86 copolymers also facilitate one-step melt mixing at a 5 wt% level with PS/PCL blends.

Fig. 8 compares the morphologies of 80/20 wt% PS/PCL blends containing 5 wt% B81, BR87, or BG86 to those of a 80/20 wt% PS/PCL blend without copolymer before and after static annealing at 210 °C for 240 min. Table 3 and Fig. 9 indicate the values of average dispersed-phase domain sizes as a function of static annealing time and copolymer type.

Several points are evident from comparison of Figs. 8 and 9 and Table 3 with Figs. 3 and 5 and Table 2. First, the dispersed-phase domain sizes are much larger when the 80/20 wt% PS/PCL blend without added copolymer is simply melt mixed as opposed to being co-dissolved, precipitated and then melt mixed. This is evident from the $D_n(0)$ values for the blends with no added copolymer: 4.80 μm for the blend made by one-step melt mixing, and 2.92 μm for the blend made by the two-step approach. This is an indication of the effectiveness of the first co-dissolution step in the two-step method in achieving a well-mixed blend.

Second, in spite of this difference, the two blends made by different methods and lacking copolymer have similar coarsening rate constants, with $K = 0.28\ \mu m^3/min$ for the blend made by the one-step method and $K = 0.22\ \mu m^3/min$ for the blend made by the two-step method. Given that each K value is obtained from fits each involving only four data points, the K values may be considered to be the same within error. This outcome is expected based on the fact that, other things being equal, K is not function of the size of the dispersed-phase domains [78].

Third, with blends made by one-step melt mixing, adding 5 wt% BG86 blocky gradient copolymer yields the smallest value of $D_n(0)$ (360 nm), a factor of 13–14 smaller than that obtained without copolymer. The addition of 5 wt% BR87 blocky random copolymer leads to a factor of 5 reduction in $D_n(0)$, and the addition of 5 wt% B81 diblock copolymer results in a 70–75% reduction in $D_n(0)$ relative to that obtained without copolymer. This ordering of initial, average dispersed-domain size and copolymer structure may be understood in part based on the effect of sequence distribution of H-bonding groups on H-bonding efficiency. Intra-association [82–84] of HS units can interfere with the ability to form inter-association H-bonds between HS units in a copolymer and PCL carbonyl groups. If intra-association is favored in copolymers containing long HS sequences, then the BR87 and BG86 copolymers, which have S units as 'spacers' between HS units, should lead to less intra-association and more interpolymer H-bonding. We note that Lin et al. [85] performed a related study with random and block copolymers of HS/methyl methacrylate (MMA) in which they characterized intra-association (HS···HS) and inter-association (HS···MMA) H-bonds. They found that random HS/MMA copolymers exhibit a higher fraction of inter-associated HS units (relative to those participating in intra-association) than HS/MMA block copolymers. (For discussion on the importance of spacer units in HS copolymers to enhance intermolecular H-bonding in blends, see Refs. [51,61,82–84].) The smaller $D_n(0)$ value observed in the blend containing BG86 relative to the blend containing BR87 may occur because a gradient distribution of HS units yields greater H-bonding at the end of the copolymer and thereby better anchoring of BG86 in PCL domains.

Finally, regarding compatibilization, addition of BR87 copolymer yields a blend that exhibits coarsening over the full 240 min annealing time with a value of the coarsening rate constant K (0.0092 $\mu m^3/min$) that is strongly reduced relative to the K value for the blend without copolymer (0.28 $\mu m^3/min$). While this reduction in K is substantial, it nevertheless indicates that addition of a block copolymer with one block consisting of a random distribution of H-bonding units does not yield compatibilization. In contrast, addition of BG86 with a block consisting of an S/HS gradient copolymer leads to a fully compatibilized blend that, within error, exhibits no coarsening during high-temperature static annealing while addition of B81 with a short HS block to the blend leads to a blend that exhibits coarsening only during the first 30 min of high-temperature static annealing. (Using data in Table 3, the blend containing BG86 exhibits a K value of 0.00011 $\mu m^3/min$, a factor of 2500 smaller than that in blend without copolymer. Thus, to an excellent approximation, K is zero in the blend containing BG86.)

In addition to 80/20 wt% blends, we also prepared 90/10 wt% PS/PCL blends with and without 5 wt% BG86 copolymer. The 90/10 wt% PS/PCL blend without copolymer yields $D_n(0) = 1.7\ \mu m$ before annealing, a factor of 2.8 smaller than that of the 80/20 wt% blend without copolymer. With addition of 5 wt% BG86, the 90/10 wt% PS/PCL blend yields $D_n(0) = 300$ nm, approaching but not at the nanoscale. With annealing at 210 °C for 240 min, the 90/10 wt% blend with BG86 exhibits a K value identical to that observed in the 80/20 wt% blend with BG86 and thus, to an excellent approximation, equivalent to zero.

The compatibilization achieved by adding 5 wt% BG86 to 80/20 wt% and 90/10 wt% PS/PCL blends indicates that the sequence distribution of HS units in the copolymer is a key feature in compatibilization efficiency involving H-bonding. While it is known that random copolymers do not fully compatibilize immiscible blends [86], even when H-bonding is present [34], this is the first study to demonstrate that a copolymer consisting of a block of one non-H-bonding unit (S) and a second, short block that is a random copolymer of non-H-bonding (S) and H-bonding (HS) units leads to reduced coarsening rather than full compatibilization. This result is especially noteworthy because an S/HS random copolymer with a composition similar to the S/HS random block in BR87 was found to be fully miscible with PCL homopolymer [55]. The inferior compatibilization efficiency of B81 block copolymer relative to BG86 gradient copolymer may be due in part to intra-association

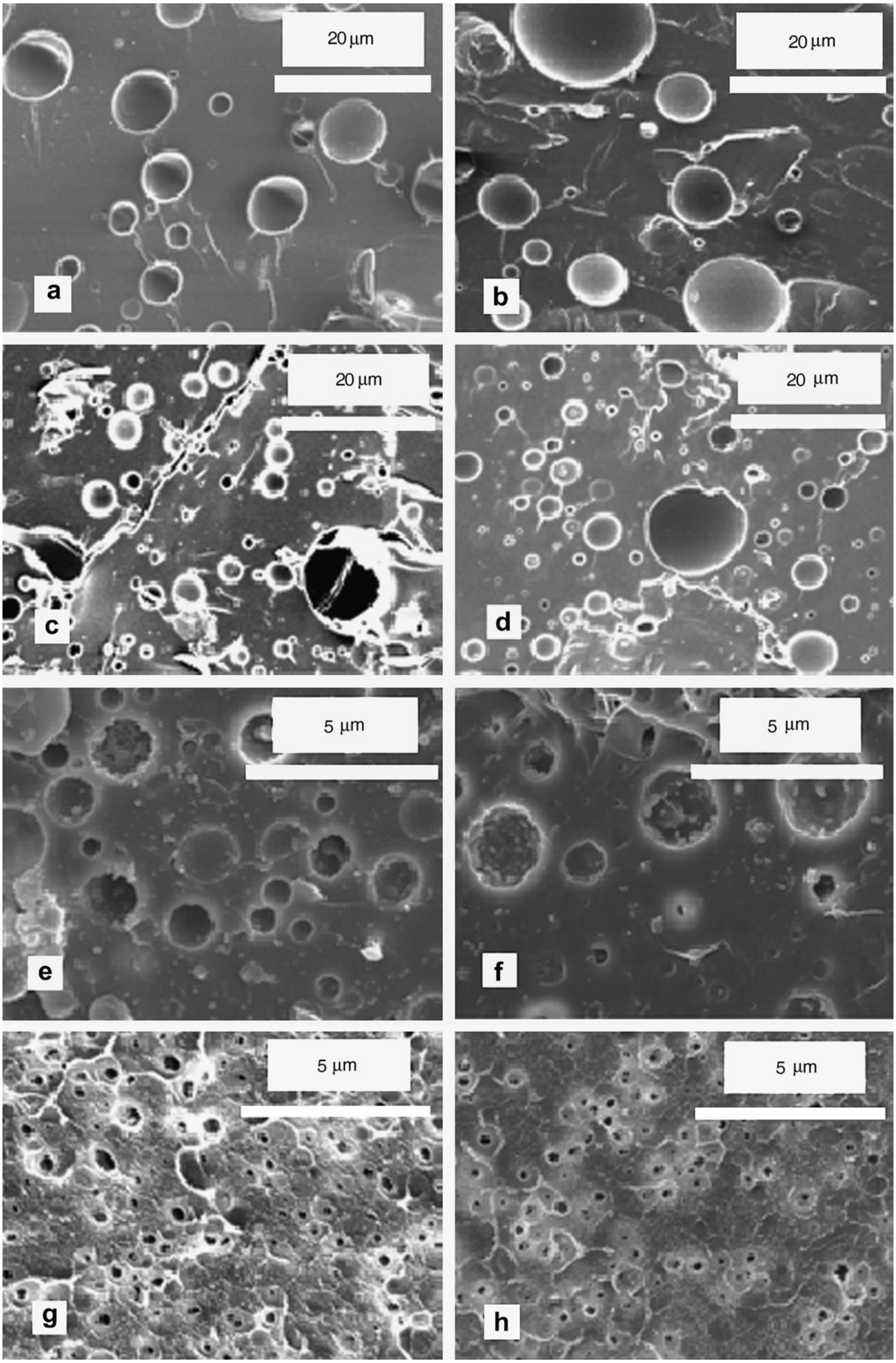

Fig. 8. Scanning electron micrographs of 80/20 wt% PS/PCL blends with or without 5 wt% addition of various types of S/HS copolymers before and after annealing for 240 min at 210 °C: blend without copolymer addition before (a) and after (b) annealing; blend with 5 wt% B81 before (c) and after (d) annealing; blend with 5 wt% BR87 before (e) and after (f) annealing; blend with 5 wt% BG86 before (g) and after (h) annealing. The size bars in (a)–(d) represent 20 μm, while those in (e)–(h) correspond to 5 μm.

effects [81–85] described above. In addition, the gradient in HS units in the short gradient block of BG86 should result in a driving force for the S/HS block to penetrate into the PCL domain interior in a manner conducive to high interfacial coverage by the copolymer, leading to effective compatibilization. It is also possible that the B81 block copolymer may not be as optimally dispersed in the blend by

Table 3
Average PCL domain sizes obtained via SEM image analysis in 80/20 wt% PS/PCL blends with 5 wt% addition of S/HS copolymers: effects of annealing time at 210 °C and type of S/HS copolymer

Added S/HS copolymer (5 wt%)	0 min annealing		30 min annealing		100 min annealing		240 min annealing	
	D_n (μm)	D_{vs}/D_n	D_n (μm)	D_{vs}/D_n	D_n (μm)	D_{vs}/D_n	D_n (μm)	D_{vs}/D_n
No copolymer	4.80	2.50	5.04	2.30	5.12	2.30	5.67	2.80
B81	1.30	2.83	2.00	4.24	1.83	4.63	1.86	3.05
BR87	0.81	2.64	0.95	2.85	1.20	2.67	1.40	2.74
BG86	0.36	1.10	0.36	1.10	0.40	1.20	0.42	1.30

melt mixing as the BR87 and BG86 copolymers because of its weak T_g at 190 °C, thereby resulting in a lower interfacial coverage of the B81 copolymer relative to the BG86 copolymer. Table 3 shows that at every annealing time the D_{vs}/D_n values are largest in the blend containing B81, which is consistent with the notion that the interfacial coverage is the least effective and the most uneven among the three copolymers used in blends made by one-step melt mixing.

Fig. 10 shows the non-isothermal crystallization and melting behaviors of PCL domains in blends made by one-step melt mixing. The thermal analyses are in accord with the morphology studies, i.e., one-step melt-mixed blends that exhibit large reductions in $D_n(0)$ values also exhibit large crystallization/melting effects. Adding 5 wt% B81 to a blend has marginal impact on PCL crystallization/melting as the magnitude and location of crystallization/melting peaks are similar to those of a melt-mixed PS/PCL blend without copolymer. In contrast, adding 5 wt% BR87 or BG86 to a blend reduces both the peak PCL crystallization temperature and the area under the crystallization peak, with a larger effect seen with BG86 addition. These results can be explained based on H-bonding resulting in a reduced crystallization of the PCL domains. However, adding BR87 or BG86 to a blend made by one-step mixing does not affect the PCL crystallization/melting behavior as severely as adding B56 to a blend by two-step mixing, as shown in Fig. 6.

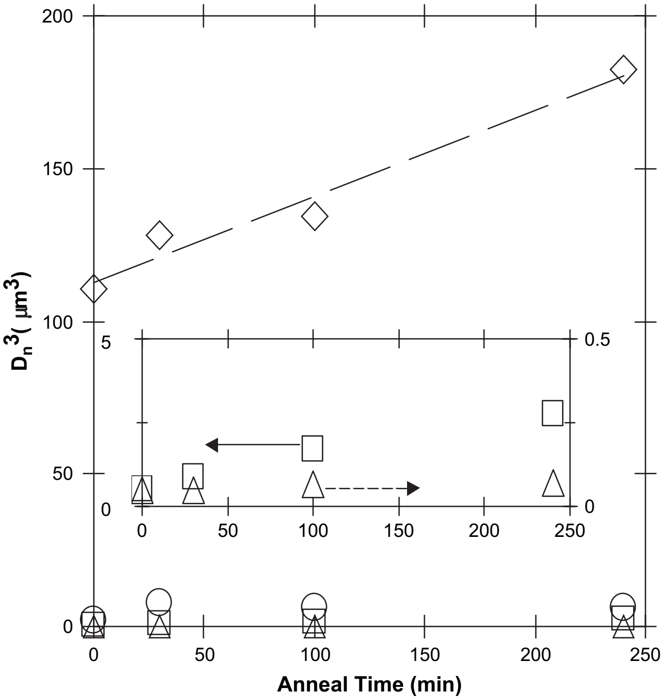

Fig. 9. Effect of annealing time on D_n^3 for 80/20 wt% PS/PCL blends shown in Fig. 8: blend without copolymer (diamonds), blend with 5 wt% B81 addition (circles), blend with 5 wt% BR87 addition (squares), and blend with 5 wt% BG86 addition (triangles). Note: The straight line represents the best fit to Eq. (1) for the blend without copolymer. The inset is a magnification of the results from BR87 addition (referred to the left axis; squares) and BG86 addition (referred to the right axis; triangles).

This is likely because the crystallizability in the blend containing B56 is reduced by combined H-bonding and confined crystallization effects, the latter associated with the ~100 nm PCL domains. (Recall that a 20/80 wt% PS/PCL blend with 5 wt% B56 made via one-step melt mixing does not allow for good mixing of the copolymer in the blend and thus shows no changes in PCL crystallization behavior.) In contrast, blends containing BR87 or BG86 (and made by one-step mixing) have dispersed domains significantly larger than ~100 nm; thus, while H-bonding retards crystallization in these blends, confined crystallization plays only a very small role in their crystallization/melting behaviors.

PS/PCL (90/10 wt%) blends show behavior similar to that of 80/20 wt% PS/PCL blends. Upon addition of 5 wt% BG86, the crystallization temperature is reduced and the peak broadens (data not shown) relative to PCL crystallization in the 90/10 wt% blend without copolymer. However, the PCL melting temperatures in all 90/10 wt% and 80/20 wt% PS/PCL blends are similar, suggesting that PCL forms crystals of comparable lamellar thickness in all blend samples.

Finally, we note that although PCL domain sizes are similar in the compatibilized 80/20 wt% PS/PCL blends containing 2 wt% B56 (made by two-step mixing) or 5 wt% BG86 (made by one-step mixing), the crystallizability is reduced to a greater extent in the blend with 2 wt% B56. This indicates that suppression of PCL crystallization in compatibilized PS/PCL blends with added S/HS copolymers is affected not only by the size scale of PCL domains but also by how the H-bonding between HS units and PCL impedes crystallization. Further investigation is needed to understand these effects in detail.

The results of our study showing the ease by which one-step melt mixing of a H-bonding blocky gradient copolymer with PS and PCL can yield compatibilized blends with dispersed domains approaching but not at the nanoscale suggest the need for future investigation. In particular, study should be done to determine whether blocky gradient or related copolymers containing H-bonding moieties or other moieties leading to attractive interactions with a homopolymer can be designed to yield compatibilized, *nanostructured* blends using one-step melt mixing. Among the copolymer design issues that are worthy of investigation and can be relatively easily addressed via controlled radical polymerization include the following: strength of the composition gradient within the gradient block; polydispersity of the blocky gradient copolymer, including molecular weight and copolymer composition; the magnitude of attractive interactions between the copolymer and homopolymer by judicious choice of comonomer units. If successful, such studies could lead to commercially attractive production of nanoblends via conventional, non-reactive melt processing.

4. Summary

Four S/HS copolymers bearing an S 'block' have been synthesized by controlled radical polymerization of S/AS followed by hydrolysis. Regardless of the distribution of S/HS units along the second block, the bulk S/HS copolymers exhibit signatures of ordered nanophases as demonstrated by the presence of two T_gs from each copolymer.

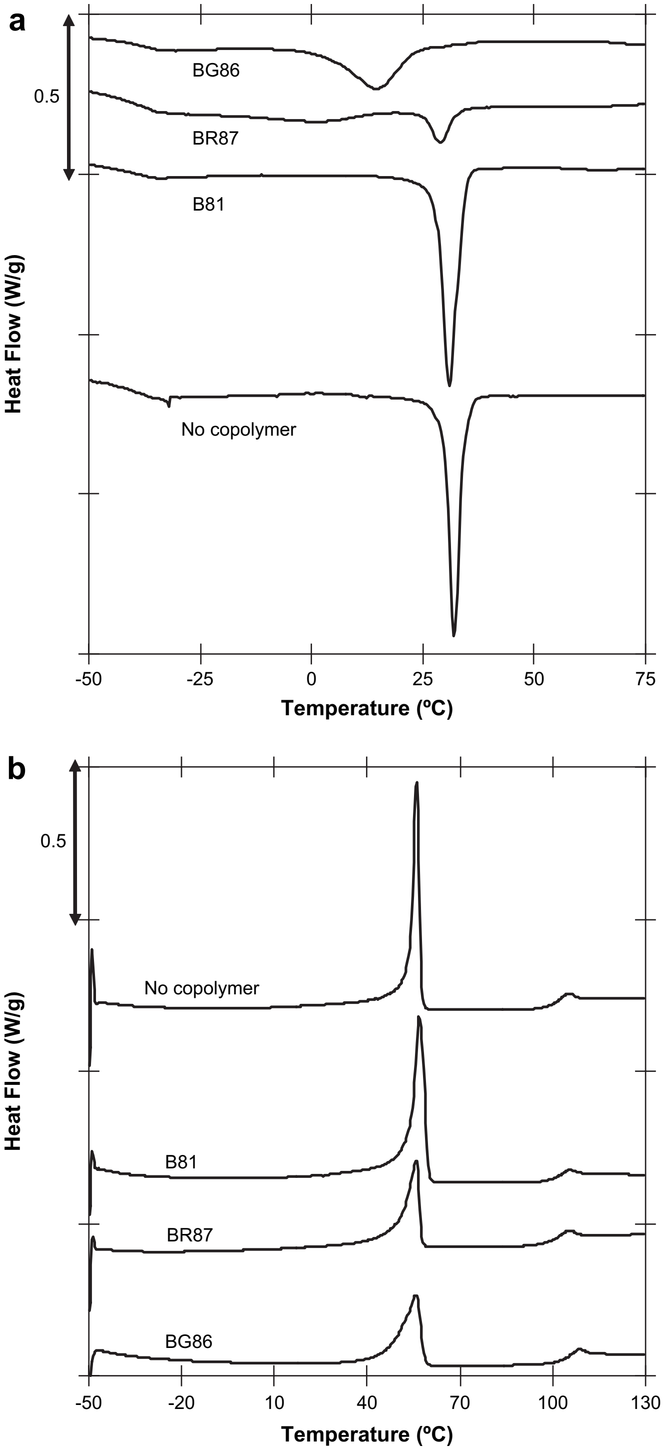

Fig. 10. DSC thermograms associated with non-isothermal crystallization (a) of PCL domains in the 80/20 wt% PS/PCL blends with or without 5 wt% of various S/HS copolymers, and melting thermograms (b) that immediately followed the non-isothermal crystallization measurements. The cooling and heating rates were 10 °C/min.

Addition of these copolymers has been investigated as a compatibilization strategy for immiscible 80/20 wt% PS/PCL blends with the HS units along the copolymer being capable of forming H-bonds with carbonyl groups in dispersed PCL domains. Depending on S/HS copolymer composition and sequence distribution, compatibilization can be achieved as evidenced by the absence of coarsening of the average dispersed-phase domain diameter during long-time high-temperature static annealing. In particular, PS/PCL blends containing 2–5 wt% (but not 0.25–0.75 wt%) of the nearly symmetric S/HS diblock copolymer B56 and made by two-step melt processing exhibit both compatibilization and very small average diameters of dispersed PCL domains (D_n), less than 500 nm with 2 wt% B56 and at the nanoscale (90–110 nm) with 5 wt% B56. Due to nanoscale confinement of PCL domains combined with H-bonding effects, the compatibilized PS/PCL nanoblends exhibit dramatically reduced PCL crystallizability. Specifically, a PS/PCL blend with 5 wt% B56 has negligible crystallinity at room temperature, meaning that the PS/PCL nanoblends contain PCL domains that are in a liquid rather than semi-crystalline state. This shows how nanostructured blends can have very different properties from microstructured blends.

The HS sequence distribution units also plays a key role in compatibilization when S/HS copolymers have low HS content. While one-step melt mixing of an 80/20 wt% PS/PCL blend with 5 wt% asymmetric diblock copolymer B81 or blocky random copolymer BR87 does not yield full compatibilization, adding 5 wt% blocky gradient copolymer BG86 yields a sub-microscale, compatibilized blend with $D_n \approx 400$ nm. Interestingly, although average PCL domain size is similar in PS/PCL blends containing 2 wt% B56 (made by two-step mixing) and 5 wt% BG86 (made by one-step mixing), the PCL crystallizability is more significantly reduced in the former case. This indicates that the suppression of PCL crystallization in compatibilized PS/PCL blends with added S/HS copolymers is affected not only by the size of PCL domains but also by the details of H-bonding between HS units along the S/HS copolymers and PCL units.

Acknowledgments

The support of the NSF-MRSEC program (Grant DMR-0076097 and Grant DMR-0520513), Northwestern University, and a 3M Fellowship (to JK) are gratefully acknowledged. We also acknowledge the use of the field-emission scanning electron microscope in a shared user facility of the Northwestern University Materials Research Center.

References

[1] Wu SH. Polymer 1985;26:1855–63.
[2] Bartczak Z, Argon AS, Cohen RE, Weinberg M. Polymer 1999;40:2331–46.
[3] Koning C, van Duin M, Pagnoulle C, Jerome R. Prog Polym Sci 1998;23:707–57.
[4] Harrats C, Thomas S, Groeninckx G. Micro- and nanostructured multiphase polymer blend systems: phase morphology and interfaces. New York: Taylor & Francis; 2006.
[5] Shimizu H, Li YJ, Kaito A, Sano H. Macromolecules 2005;38:7880–3.
[6] Hu GH, Feng LF. Macromol Symp 2003;195:303–8.
[7] Pernot H, Baumert M, Court F, Leibler L. Nat Mater 2002;1:54–8.
[8] Leibler L. Prog Polym Sci 2005;30:898–914.
[9] Alam TM, Otaigbe JU, Rhoades D, Holland GP, Cherry BR, Kotula PG. Polymer 2005;46:12468–79.
[10] Zinck P, Brachais CH, Finot E, Barbier-Baudry D. Macromol Chem Phys 2005; 206:553–8.
[11] Chan SH, Lin YY, Ting C. Macromolecules 2003;36:8910–2.
[12] Tao Y, Kim J, Torkelson JM. Polymer 2006;47:6773–81.
[13] Macosko CW, Guegan P, Khandpur AK, Nakayama A, Marechal P, Inoue T. Macromolecules 1996;29:5590–8.
[14] Sundararaj U, Macosko CW. Macromolecules 1995;28:2647–57.
[15] Grace HP. Chem Eng Commun 1982;14:225–77.
[16] Taylor GI. Proc R Soc London 1934;A146:501–23.
[17] Lebovitz AH, Khait K, Torkelson JM. Polymer 2003;44:199–206.
[18] Tol RT, Mathot VBF, Groeninckx G. Polymer 2005;46:383–96.
[19] Wildes G, Keskkula H, Paul DR. J Polym Sci Part B Polym Phys 1999;37:71–82.
[20] Kim HY, Jeong U, Kim JK. Macromolecules 2003;36:1594–602.
[21] Maric M, Ashurov N, Macosko CW. Polym Eng Sci 2001;41:631–42.
[22] Lebovitz AH, Khait K, Torkelson JM. Macromolecules 2002;35:8672–5.
[23] Lebovitz AH, Khait K, Torkelson JM. Macromolecules 2002;35:9716–22.
[24] Kim HC, Nam KH, Jo WH. Polymer 1993;34:4043–51.
[25] Auschra C, Stadler R, Voigt-Martin IG. Polymer 1993;34:2081–93.
[26] Anastasiadis SH, Gancarz I, Koberstein JT. Macromolecules 1989;22:1449–53.
[27] Tao Y, Lebovitz AH, Torkelson JM. Polymer 2005;46:4753–61.
[28] Fayt R, Jerome R, Teyssie P. J Polym Sci Part B Polym Phys 1982;20:2209–17.
[29] Harrats C, Fayt R, Jerome R, Blacher S. J Polym Sci Part B Polym Phys 2003;41: 202–16.

[30] Laurer JH, Smith SD, Samseth J, Mortensen K, Spontak RJ. Macromolecules 1998;31:4975–85.
[31] Jannasch P, Wesslen B. J Appl Polym Sci 1995;58:753–70.
[32] Gonzalez-Montiel A, Keskkula H, Paul DR. J Polym Sci Part B Polym Phys 1995; 33:1751–67.
[33] Kim J, Gray MK, Zhou HY, Nguyen ST, Torkelson JM. Macromolecules 2005;38: 1037–40.
[34] Kim J, Zhou HY, Nguyen ST, Torkelson JM. Polymer 2006;47:5799–809.
[35] Pakula T, Matyjaszewski K. Macromol Theory Simul 1996;5:987–1006.
[36] Matyjaszewski K, Ziegler MJ, Arehart SV, Greszta D, Pakula T. J Phys Org Chem 2000;13:775–86.
[37] Jose S, Francis B, Thomas S, Karger-Kocsis J. Polymer 2006;47:3874–88.
[38] Kobori Y, Akiba I, Akiyama S. Polymer 2000;41:5971–5.
[39] Kobori Y, Yasumitsu R, Akiba I, Akiyama S, Sano H. e-Polymers 2004;4:1–6.
[40] Watanabe N, Akiba I, Akiyama S. Eur Polym J 2001;37:1837–42.
[41] Xu ZH, Kramer EJ, Edgecombe BD, Frechet JMJ. Macromolecules 1997;30:7958–63.
[42] Edgecombe BD, Stein JA, Frechet JMJ, Xu ZH, Kramer EJ. Macromolecules 1998; 31:1292–304.
[43] Mekhilef N, Favis BD, Carreau PJ. J Polym Sci Part B Polym Phys 1997;35: 293–308.
[44] Gray MK, Zhou HY, Nguyen ST, Torkelson JM. Macromolecules 2004;37: 5586–95.
[45] Mok MM, Kim J, Torkelson JM. J Polym Sci Part B Polym Phys 2008;46:48–58.
[46] Kim J, Mok MM, Sandoval RW, Woo DJ, Torkelson JM. Macromolecules 2006; 39:6152–60.
[47] Georges MK, Veregin RPN, Kazmaier PM, Hamer GK. Macromolecules 1993;26: 2987–8.
[48] Davis KA, Matyjaszewski K. Adv Polym Sci 2002;159:1–169.
[49] Vidts KRM, Dervaux B, Du Prez FE. Polymer 2006;47:6028–37.
[50] Zheng RH, Liu GJ, Jao TC. Polymer 2007;48:7049–57.
[51] Coleman MM, Painter PC. Prog Polym Sci 1995;20:1–59.
[52] He Y, Zhu B, Inoue Y. Prog Polym Sci 2004;29:1021–51.
[53] Ahn TO, Eum HS, Jeong HM, Park JY. Polym Bull 1993;30:461–7.
[54] Lezcano EG, Coll CS, Prolongo MG. Polymer 1996;37:3603–9.
[55] Vaidya MM, Levon K, Pearce EM. J Polym Sci Part B Polym Phys 1995;33: 2093–108.
[56] Zhou H, Xiang ML, Chen WJ, Jiang M. Macromol Chem Phys 1997;198:809–17.
[57] Chen HL, Wang SF, Lin TL. Macromolecules 1998;31:8924–30.
[58] Kuo SW, Chang FC. Macromolecules 2001;34:7737–43.
[59] Landry CJT, Teegarden DM. Macromolecules 1991;24:4310–21.
[60] Wang J, Cheung MK, Mi YL. Polymer 2002;43:1357–64.
[61] Viswanathan S, Dadmun MD. Macromolecules 2002;35:5049–60.
[62] Jong L, Pearce EM, Kwei TK. Polymer 1993;34:48–55.
[63] Demeftahi MV, Frechet JMJ. Polymer 1988;29:477–82.
[64] Xu Y, Graf J, Painter PC, Coleman MM. Polymer 1991;32:3103–18.
[65] Zhao JQ, Pearce EM, Kwei TK. Macromolecules 1997;30:7119–26.
[66] Zeng XM, Weng LT, Li L, Chan CM, Liu SY, Jiang M. Surf Interface Anal 2001;31: 421–8.
[67] Loo YL, Register RA, Ryan AJ, Dee GT. Macromolecules 2001;34:8968–77.
[68] Reiter G, Castelein G, Sommer JU, Rottele A, Thurn-Albrecht T. Phys Rev Lett 2001;87:226101.
[69] Tol RT, Mathot VBF, Groeninckx G. Polymer 2005;46:2955–65.
[70] Frensch H, Harnischfeger P, Jungnickel BJ. ACS Symp Ser 1989;395:101–25.
[71] Muller AJ, Balsamo V, Arnal ML, Jakob T, Schmalz H, Abetz V. Macromolecules 2002;35:3048–58.
[72] Huang P, Guo Y, Quirk RP, Ruan JJ, Lotz B, Thomas EL, et al. Polymer 2006;47: 5457–66.
[73] Jones BA, Torkelson JM. J Polym Sci Part B Polym Phys 2004;42:3470–5.
[74] Benoit D, Chaplinski V, Braslau R, Hawker CJ. J Am Chem Soc 1999;121: 3904–20.
[75] Maric M, Macosko CW. Polym Eng Sci 2001;41:118–30.
[76] Brandrup J. In: Brandrup J, Immergut EH, Grulke EA, Abe A, Bloch DR, editors. Polymer handbook. 4th ed. New York: Wiley; 1999. p. 263 [Section II].
[77] Still RH, Whitehead A. J Appl Polym Sci 1977;21:1215–25.
[78] Crist B, Nesarikar AR. Macromolecules 1995;28:890–6.
[79] Siggia ED. Phys Rev A 1979;20:595–605.
[80] Song SW, Torkelson JM. Macromolecules 1994;27:6389–97.
[81] Xing PX, Dong LS, An YX, Feng ZL, Avella M, Martuscelli E. Macromolecules 1997;30:2726–33.
[82] Coleman MM, Pehlert GJ, Painter PC. Macromolecules 1996;29:6820–31.
[83] Painter PC, Veytsman B, Kumar S, Shenoy S, Graf JF, Xu Y, et al. Macromolecules 1997;30:932–42.
[84] Pehlert GJ, Painter PC, Veytsman B, Coleman MM. Macromolecules 1997;30: 3671–7.
[85] Lin CL, Chen WC, Liao CS, Su YC, Huang CF, Kuo SW, et al. Macromolecules 2005;38:6435–44.
[86] Lee MS, Lodge TP, Macosko CW. J Polym Sci Part B Polym Phys 1997;35: 2835–42.